PERGAMON

Journal of Structural Geology 22 (2000) 245–258

JOURNAL OF STRUCTURAL GEOLOGY

www.elsevier.nl/locate/jstrugeo

The relationship of phyllosilicate orientation, X-ray diffraction intensity ratios, and *c*/*b* fissility ratios in metasedimentary rocks of the Helvetic zone of the Swiss Alps and the Caledonides of Jämtland, central western Sweden

Gerd Jacob[a,*], Hanan J. Kisch[b], Ben A. van der Pluijm[c]

[a]*Department of Geological Sciences, University of Halle, Domstr.5, 06108 Halle, Germany*
[b]*Department of Geology & Mineralogy, Ben-Gurion University of the Negev, P.O.B. 653, Beer-Sheva 84 105, Israel*
[c]*Department of Geological Sciences, University of Michigan, 2534 C.C. Little Building, Ann Arbor, MI 48109-1063, USA*

Received 7 September 1998; accepted 7 September 1999

Abstract

Phyllosilicate preferred orientations, X-ray diffraction intensity ratios, and *c*/*b* fissility ratios were determined from 23 metasedimentary rocks from the Helvetic zone of the Swiss Alps and from the Caledonides of Jämtland, Sweden. The relationships between these parameters of phyllosilicate orientation depend strongly on the lithology and the cleavage morphology. Differences in orientation direction and in degree of preferred orientation reflect both deformation intensities and lithologies. Whereas polyphase deformed, fine-grained samples generally have phyllosilicates that are oriented parallel to cleavage showing high orientation intensities, phyllosilicates in less deformed and/or coarse-grained rocks are oriented parallel to bedding with low orientation intensities. Weak orientation intensities in samples with phyllosilicates that are oriented parallel to bedding reflect compaction strain. The higher strain in samples with micas and chlorites that are parallel to cleavage is a combination of compaction and tectonic strain due to the development of crenulation cleavage.

1. Introduction

The preferred crystallographic orientation of phyllosilicates in argillaceous rocks reflects the strain and the degree of reorientation of platy minerals during cleavage formation in these rocks. The importance of the development of preferred orientations of phyllosilicates, particularly of mica and chlorite, has been studied by many authors to investigate mechanisms of cleavage development (Holleywell and Tullis, 1975; Ho et al., 1995, 1996) or to estimate finite strain (Chen and Oertel, 1980; Oertel, 1983; Oertel et al., 1989). Cleavage development in pelites is closely related to the development of phyllosilicate preferred orientations (Ramsay and Huber, 1983). Phyllosilicate pole figure measurement is one of only a few ways to represent strain in pelitic rocks, and the determination of phyllosilicate preferred orientation also allows a quantification of the degree of cleavage development (Sintubin, 1994a).

The determination of the preferred orientation of phyllosilicates is generally done by X-ray goniometry. Although the latter method has specific advantages (suitable for a wide range of minerals, rapid determination of orientations, large number of grains), it requires special equipment (special stage—see van der Pluijm et al., 1994), and so is not universally available. Kisch (1994, 1998) combined the measurement of X-ray diffraction intensity ratios of the (001)-reflections

* Corresponding author.
E-mail addresses: jacob@geologie.uni-halle.de (G. Jacob), kisch@bgumail.bgu.ac.il (H.J. Kisch), vdpluijm@umich.edu (B.A. van der Pluijm).

0191-8141/00/$ - see front matter
PII: S0191-8141(99)00149-2

of white mica, and the (002)-reflection of chlorite in cleavage- and bedding-parallel slabs with the dimensional aspect ratios of fissility fragments (the cleavage/bedding fissility ratios after Durney and Kisch, 1994) to establish combined criteria for a quantitative description of incipient slaty cleavage. Both the X-ray intensity ratios and the c/b fissility ratios reflect relative cleavage intensities, but they do not relate exactly to the same aspect of the fabric. The X-ray intensity ratio provides information about the orientation of phyllosilicates during the development of cleavage fabrics, and about the relative formation of illite and chlorite in cleavage domains and in chlorite-mica aggregates. The fissility ratios depend on both the overall phyllosilicate orientation and the cleavage microstructure, particularly on the morphology and on the spacing of cleavage domains, and on the intensity of a bedding-parallel cleavage fabric in the microlithons of rocks with a crenulation cleavage.

The purpose of this paper is to compare results of phyllosilicate preferred orientation measurements with X-ray diffraction intensity ratios and c/b fissility ratios measured on a series of metasediments of various stratigraphical positions, and from different locations (Tertiary flysch of the Helvetic Alps, and Ordovician and Silurian metasediments of the Caledonides of Jämtland, western central Sweden). The intensities of phyllosilicate preferred orientation will be used to verify different parameters of cleavage intensities, such as X-ray intensity ratios and cleavage/bedding fissility ratios.

2. Sample locations and descriptions

Samples were selected from suites of rocks collected from Tertiary flysch of the Helvetic Alps and from Ordovician to Silurian series of the Jämtlandian nappes (lower Allochthon) of the external Caledonides of Jämtland Province, western central Sweden. The sample localities are listed in Table 1 (see also Kisch, 1980, 1994, 1998).

The localities in the Helvetic Alps are part of the Infrahelvetic complex; i.e. all units underlying the Glarus thrust, which is the basal thrust of the Helvetic nappe system (Milnes and Pfiffner, 1977; Arkai et al., 1997; Pfiffner, 1978). Most of the samples are from the Subhelvetic Griesstock Nappe and the Upper Eocene to Lower Oligocene parautochthonous North Helvetic Flysch (*area 1* — Linthal–Urnerboden–upper Schächental–Trübsee of Kisch, 1998).

The samples of the Swiss Alps represent a suite of fine, silty shales, mudstones and slaty, marly claystones with a smooth incipient slaty or crenulation cleavage. The crenulation cleavage is predominantly discrete, but in most samples the micas in the margins of the microlithons show deflection into the cleavage domains, giving them diffuse boundaries (zonal crenulation cleavage in the sense of Gray, 1977). The crenulated fabric is an earlier penetrative slaty S_1-cleavage, which is bedding-parallel in most cases (Kisch, 1998).

The Swedish samples were collected from the Ordovician Föllinge Graywacke Formation and one (N92-7) from the Middle Silurian Röde Sandstone Formation, from two anchimetamorphic areas in the internal part of the Föllinge Nappe (Asklund and Thorslund, 1935)—the Mörsil–Järpen–Bångåsen area to the south and the Föllinge area to the north. One additional sample (N78-59B) was studied from the Middle Ordovician Andersön Shale on Norderön island in the low-grade anchizone of the external underlying lower thrust sheets of the southeastern Storsjön area (Sunne Nappe of Thorslund, 1940 and Frösön Allochthon or Frösön Nappe of Gee and Kumpulainen, 1980).

With three exceptions, all of the samples of the Swedish Caledonides are mudstones and siltstones with almost no, or only a very incipient, crenulation cleavage. The siltstones show a domainal, discontinuous sometimes anastomosing cleavage, whereas the finer mudstones (N78-8A, 59B, N92-15D, 17A), and the three claystone samples (N92-15G, 18B, 20) show an incipient crenulation cleavage. The crenulation cleavage in these samples is predominantly zonal; some of the clastic micas at the margins of the cleavage domains are rotated and sigmoidally deformed. There is no crenulation cleavage in the coarser grained siltstones (N78-7, 44B, 47A, N92-6, 18A) or in the sandy siltstone (N92-15F). Only irregular, discontinuous cleavage domains and poorly marked bedding fabrics were found. There is no significant crystallization of mica in the cleavage domains, but abundant bedding-parallel clastic mica. For additional details of the lithology, cleavage type, and localities of the samples the reader is referred to Kisch (1994, 1998).

3. Methods and sample preparation

The samples were studied by optical microscopy, scanning electron microscopy (SEM) and X-ray diffraction (XRD). Cleavage/bedding fissility ratios (c/b ratio), after Durney and Kisch (1994), were determined in the field. These ratios are quantified by the measurement of the aspect ratios of fissility fragments in the cleavage direction relative to the bedding direction. The ratios are measured along the cleavage- and bedding-fabric anisotropy on the plane normal to the bedding/cleavage intersection. The measurements were made on the real cleavage and bedding directions, and then, if not perpendicular, the angle was corrected to oblique c/b values.

Table 1
Locations, lithology and cleavage type of samples

Sample No.	Locality	Lithology/size of detrital grains	Cleavage morphology
Z 91-1	1.5 km SSE of Linthal, northern end of second road tunnel	claystone/ < 10 μm	discrete and locally zonal crenulation, CDS 30–100 μm
Z 91-2A	1.5 km SSE of Linthal, northern end of second road tunnel	slaty mudstone/ < 20 μm	discrete and zonal crenulation, CDS 30–100 μm
Z 91-3	1.5 km SSE of Linthal, northern end of second road tunnel	calcareous siltstone with claystone and silty mudstone beds/ < 20 μm; in silty layers quartz-grains 20–100 μm; chlorite mica stacks ≈100 μm	discrete and zonal crenulation in claystone layers, CDS 50–100 μm; anastomosing in silty layers
Z 91-6	NE Äsch, Vorder Schächental	calcareous silty mudstone with mudstone layers/20–40 μm	domainal sinuous anastomosing in silty layers, CDS 20 μm; discontinuous anastomosing in mudstone layers, no crenulation, CDS 50 μm
Z 91-7	NE Äsch, Vorder Schächental	slaty mudstone/ < 20 μm	domainal sinuous, no crenulation, CDS 15 μm
Z 91-8	Wanneler Bach, Vorder Schächental	slaty calcareous mudstone/10–40 μm	discrete and zonal crenulation, CDS 50–100 μm
Z 91-9	Wanneler Bach, Vorder Schächental	mudstone with laminae of calcareous siltstone/ < 30 μm	zonal and some discrete crenulation in mudstone layers, CDS 40–150 μm
Z 91-10	Fritertal, N of Friteren, Vorder Schächental	calcareous slaty mudstone/10–40 μm	local zonal crenulation, CDS 30 μm
Z 91-13	SE of Trübsees, S of Engelberg	marly siltstone/20–70 μm	domainal anastomosing, no crenulation CDS 30–50 μm
N 78-5	W Föllinge	slaty mudstone, many chlorite–mica stacks/ 10–70 μm; stacks ≈100 μm	domainal anastomosing, no crenulation, CDS 50 μm
N78-7	Föllinge–Lillholmsjö	siltstone/10–70 μm	zonal, discontinuous, domainal, no crenulation, CDS 100–200 μm
N78-8A	NW Föllinge	silty mudstone/20–100 μm	discontinuous, locally zonal crenulation, CDS 50 μm
N78-44B	E Järpen	bedded silty mudstone with claystone and quartz-rich siltstone layers/ < 10 μm in claystone layers; 20–70 μm in silty layers	discontinuous anastomosing, no crenulation, CDS 70 μm
N78-47A	Mörsil–Järpen	siltstone/20–100 μm	domainal anastomosing, no crenulation, CDS ≈100 μm
N78-59B	N Norderön	slaty mudstone/10–70 μm	domainal, locally zonal crenulation, CDS 50 μm
N92-6	E Mörsil	siltstone/10–100 μm	domainal, discontinuous anastomosing, no crenulation, CDS 50–80 μm
N92-15D	W Föllinge	slaty mudstone/20–50 μm	domainal, continuous, locally zonal crenulation, CDS 30 μm
N92-15F	W Föllinge	sandy siltstone/50–250 μm	domainal, discontinuous anastomosing, no crenulation, CDS ≈200 μm
N92-15G	W Föllinge	slaty claystone/ < 10 μm	domainal, locally zonal crenulation, CDS 30 μm
N92-17A	NW Föllinge	mudstone/10–40 μm	domainal, discontinuous, locally zonal crenulation, CDS 20 μm
N92-18A	Föllinge Skärvängen	silty mudstone with layers of quartz-rich siltstone/10–100 μm	domainal, discontinuous, no crenulation, CDS 20–50 μm
N92-18B	Föllinge Skärvängen	claystone/ < 10 μm	domainal, locally zonal crenulation, CDS 20 μm
N92-20	Föllinge–Lillholmsjö	slaty claystone/ < 10 μm	domainal, locally zonal crenulation, CDS 10–20 μm

The illite crystallinities (IC; i.e. the full-width-at-half-maximum (FWHM) of the 10 Å basal reflection of illite–muscovite) were measured by X-ray diffractometry (XRD) in order to determine the metamorphic grade of the samples. The measurements were performed on slides (air-dried and Ca-saturated powder samples) of the <2 μm fraction. The measurements were carried out at the Department of Geology & Mineralogy in Beer-Sheva with a Philips generator 1730/goniometer 1050 with the following instrumental and measuring settings: Cu Kα, normal focus tube, Ni-filter, slits 1°–0.2 mm–1°, Xenon proportional detector

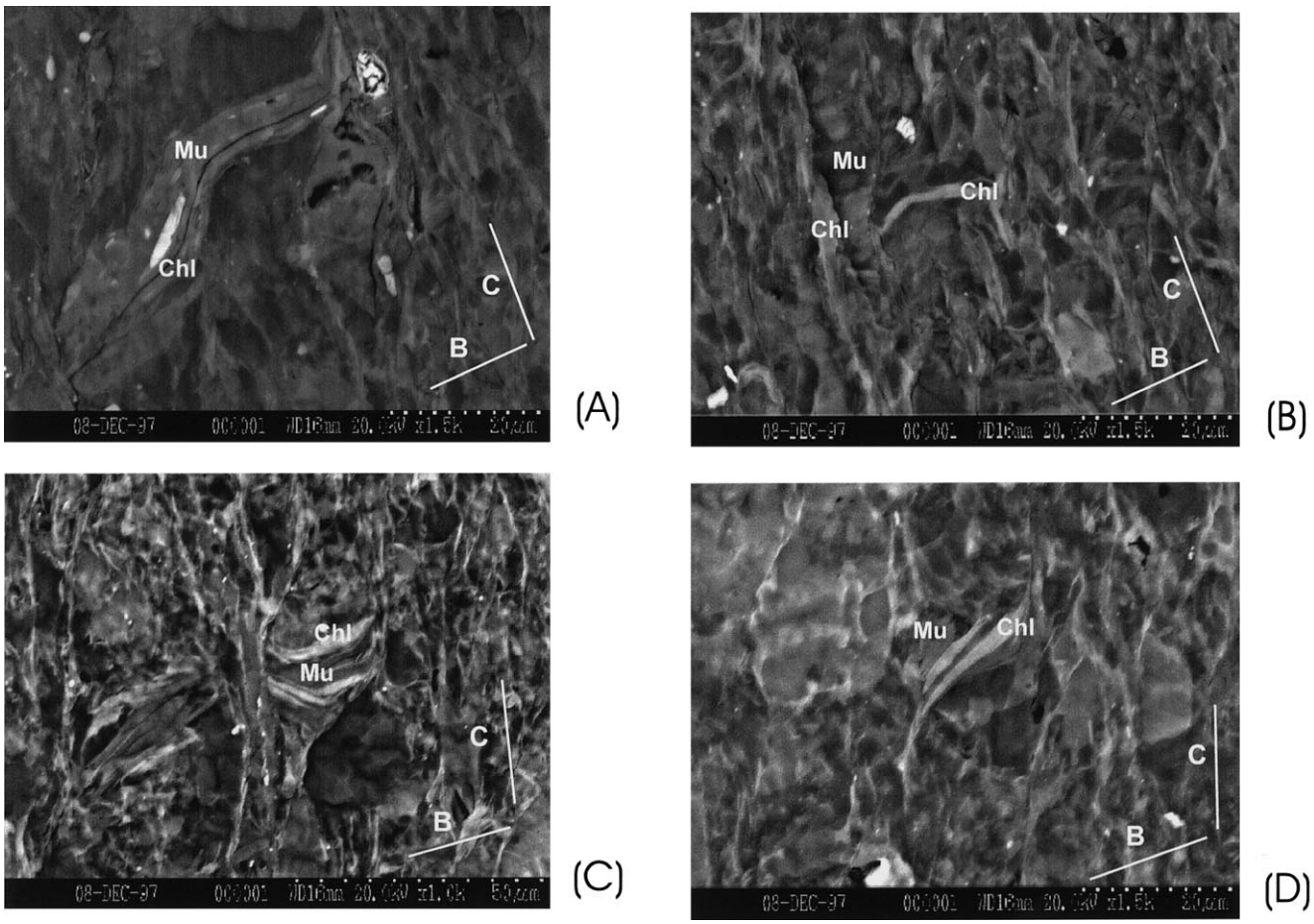

Fig. 1. Selected BSE images of samples with chlorite–mica aggregates: (A) and (B) sample Z91-13; (C) and (D) sample Z91-7. Mica (illite/muscovite – Mu), chlorite (Chl), and orientation of bedding (B), and cleavage (C) are labeled. (A) Voltage = 20.0 kV, magnification × 1.5k, scale bar = 20 μm. (B) 20.0 kV, ×1.5k, scale bar = 20 μm. (C) 20.0 kV, ×1.0k, scale bar = 50 μm. (D) 20.0 kV, ×1.5, scale bar = 20 μm. See text for discussions.

(PW 1711), T.C. = 2 sec for scan rate 0.6° 2θ/min (or T.C. = 1 sec for scan rate 1.2° 2θ/min).

The high- and low-grade limits of the anchizone correspond to 10 Å peak half-height widths of 0.21° and 0.37–0.38° $\Delta 2\theta$ (Kisch, 1980, 1990).

Polished bedding- and cleavage-parallel slabs were used for the measurements of the X-ray intensity ratios of illite/muscovite (001)-reflections. To avoid a slab-size dependent variation of the measured X-ray intensity values it is important to cut the slabs at a width of at least 18 mm (Kisch, 1994). The intensities of the low-angle reflections of mica and chlorite at 10 Å and 7 Å were measured using a divergence/scatter slit set of 0.5°. In addition these intensities were measured using a slit set of 1°. All measurements were performed without removing the slabs from the sample holder.

The crystallographic preferred orientations of phyllosilicates were measured on a modified X-ray pole figure device attached to an automated Enraf–Nonius CAD4 single-crystal diffractometer with Mo Kα-radiation source and scintillation detector. Detailed instrumentation and correction procedures are described in van der Pluijm et al. (1994) and Ho (1997).

The X-ray goniometry measurements and the SEM observations were performed on polished sections of about 200 μm thickness. The sections were cut perpendicular to both bedding and cleavage. The exact thickness of each sample was measured to calculate the X-ray absorption factors.

4. Results

4.1. SEM

Three types of phyllosilicate microstructures were observed by SEM observations:

Type 1. Fine-grained mica and chlorite in the matrix. The size of these phyllosilicate aggregates are less than 20 μm, which is too small to be resolved by SEM.

Table 2
Data for studied samples: illite crystallinities measured on fraction <2 μm, c/b fissility ratios, peak intensity ratios I10 Å (0.5°) C/B, and maximum orientation intensities for mica (001)-, chlorite (001)- and chlorite/kaolinite (002)-reflections in multiples of the random distribution (mrd) and absolute counts in the maximum

Sample No.	Illite crystallinity (<2 μm; $\Delta 2\theta$)	c/b fissility ratio	I10 Å (0.5°) C/B	Maximum intensity mica (001) (counts)	Maximum intensity mica (001) (mrd)	Maximum intensity chlorite (001) (counts)	Maximum intensity chlorite (001) (mrd)	Maximum intensity chlorite/kaolinite (002) (counts)	Maximum intensity chlorite/kaolinite (002) (mrd)
Z 91-1	0.29	2.00	2.889	242	7.08	174	7.99	393	7.85
Z 91-2A	0.31	1.00	0.488	435	9.20	254	8.88	530	6.44
Z 91-3	0.30	3.50	0.313	110	6.55	134	10.70	741	7.63
Z 91-6	0.34	3.50	0.723	371	10.43	161	13.73	358	9.68
Z 91-7	0.39	6.00	11.000	351	12.91	171	16.71	401	10.59
Z 91-8	0.30	0.33	0.440	103	7.46	60	11.96	160	8.20
Z 91-9	0.28	0.50	0.421	310	8.44	223	12.38	562	9.05
Z 91-10	0.36	–	1.894	427	12.15	200	11.33	415	9.79
Z 91-13	0.29	2.50	6.897	177	8.85	92	14.89	357	6.96
N 78-5	0.29	1.50	0.923	145	2.39	22	4.48	98	2.45
N78-7	0.30	1.25	1.390	157	3.04	65	3.48	187	2.65
N78-8A	0.27	1.00	1.240	102	2.95	38	4.05	–	–
N78-44Bf	0.25	0.67	0.799	295	8.20	131	5.64	313	5.42
N78-44Bg	0.25	0.67	0.799	24	3.70	–	–	–	–
N78-47A	0.25	2.00	2.470	142	4.08	86	8.36	289	5.34
N78-59B	0.30	1.00	1.030	200	5.47	65	12.46	249	4.36
N92-6	0.31	3.00	0.584	99	3.53	–	–	299	4.38
N92-15D	0.28	2.00	1.200	65	2.85	22	3.86	45	3.40
N92-15F	0.26	2.00	0.705	94	2.75	–	–	79	2.92
N92-15G	0.29	2.50	1.680	658	8.65	201	14.29	404	9.97
N92-17A	0.27	2.00	0.451	166	10.40	100	14.17	56	10.77
N92-18A	0.29	2.50	0.709	79	2.42	66	2.86	67	3.26
N92-18B	0.29	2.50	2.430	161	4.22	62	5.36	146	4.22
N92-20	0.30	1.75	0.335	607	7.45	280	8.70	495	8.10

Type 2. Fine-grained mica and chlorite in the cleavage domains. The grains are too small (less than 20 μm) for SEM observations. The mainly cleavage-parallel crystals are authigenic in origin. Some of these phyllosilicates were rotated during the formation of the crenulation cleavage.

Type 3. Large chlorite–mica aggregates. These stacks are variably dominated by chlorite and by muscovite/illite. The stacks are detrital or early diagenetic in origin, and at least the chlorite dominated stacks are modified biotite grains formed by replacement of biotite by chlorite during diagenesis and metamorphism, as described by Li et al. (1994).

A large proportion of the stacks consists almost entirely of chlorite with very subordinate muscovite lamellae, others have chlorite centers with muscovite margins. The mainly bedding-parallel chlorite–mica stacks show different morphologies, depending on the deformation mechanisms and the intensity of cleavage formation. In samples with incipient and less developed cleavage the aggregates are roughly rectangular or ellipsoidal, with the longest dimension parallel to the crystallographic (001)-plane of both mica and chlorite. In samples with a stronger crenulation cleavage the chlorite–mica stack aggregates are deformed and irregular in shape. The observed deformation mechanisms are mainly rigid-body rotation and intragranular kinking with external deformation of the aggregates being stronger than the internal deformation. Large and relatively thin stacks show kinking and they are cross-cut by cleavage-planes (Fig. 1b and c), whereas the thicker aggregates are rotated or dragged with respect to the shear direction on the crenulation cleavage planes (Fig. 1a and d).

4.2. Metamorphic grade—illite crystallinity

The results of the illite crystallinity (IC) measurements of the <2 μm fraction of the samples collected for this study are listed in Table 2 and are used to estimate the metamorphic grade.

The peak-width values of the Swiss samples range between 0.27 and 0.39° $\Delta 2\theta$. Using the low- and high-grade limits of the anchizone of Kisch (1980, 1990), the metamorphic grade can be determined as low- to medium-grade anchizonal with one high-grade diagenetic exception (Z91-7). Metamorphism of the samples from Jämtland is medium-grade anchizonal in the Mörsil–Järpen–Bångåsen area (0.25–0.27° $\Delta 2\theta$) and low- to medium-grade anchizonal in the Föllinge area (0.27–0.31° $\Delta 2\theta$).

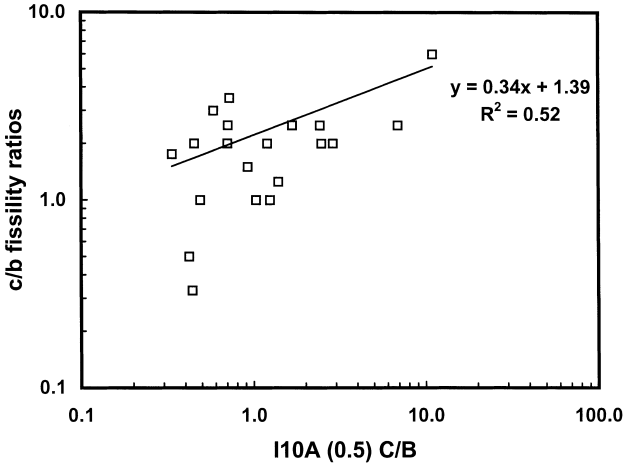

Fig. 2. Variation of the c/b cleavage/bedding fissility ratios with the I10 Å (0.5°) C/B ratios.

4.3. Phyllosilicate orientation and cleavage/bedding fissility ratio

The c/b fissility ratios as measured in the field and the I10Å (0.5°) C/B intensity ratios are shown in Table 2. The fissility ratios range from 0.30 to 6.00 for the Swiss samples and from 0.67 to 3.00 for the samples from Jämtland. The 10 Å intensity ratios range from 0.31 to 11.00 and from 0.34 to 2.47, respectively. There are no obvious differences between the values of the c/b fissility ratios of the two regions, but the I10 Å (0.5°) C/B intensity ratios of the samples of the Helvetic Alps seem to be slightly higher than those of the Jämtland samples.

The c/b fissility ratios have been plotted against the I10 Å (0.5°) C/B intensity ratios for all measured samples (Fig. 2). The plot shows a rather scattered correlation, with a regression of:

$$c/b = 0.34 \times \text{I10 Å}(0.5^\circ)C/B + 1.39 \quad (R^2 = 0.52).$$

As mentioned by Kisch (1998), a major reason for the divergence of some samples from this relationship appears to reside in the lithology of the samples. Indeed, the lithology of the investigated samples shows a relationship to the type of cleavage. Apart from the composition a major difference is the presence of an initial crenulation cleavage in all of the claystone and mudstone samples. When the coarser-grained silty samples with no crenulation cleavage are removed from consideration, a better relationship is obtained (Fig. 3):

$$c/b = 0.42\text{I10 Å} \times (0.5^\circ)C/B + 1.30 \quad (R^2 = 0.90).$$

In contrast to Kisch (1994, 1998) the marly samples show lower c/b fissility ratios for given I10 Å (0.5°) $C/$

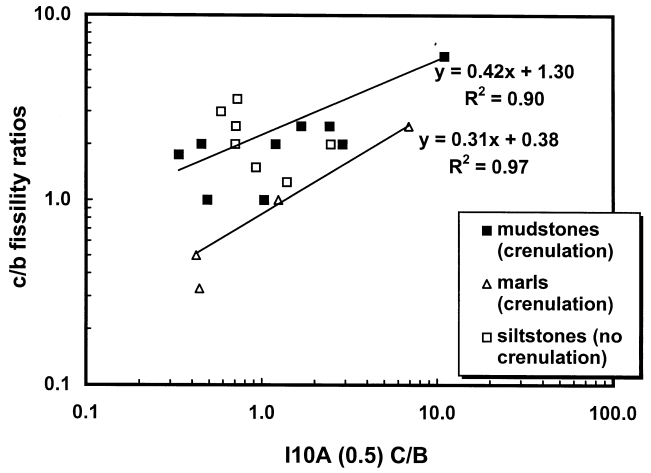

Fig. 3. Variation of the c/b cleavage/bedding fissility ratios with the I10 Å (0.5°) C/B ratios: relation to lithology and cleavage morphology.

B intensity ratios than the claystone/mudstone samples (Fig. 3).

With one exception (Z91-7) there are no significant differences between the I10 Å (0.5°) C/B intensity ratios and the c/b fissility ratios for the non-marly crenulated samples and the samples without a crenulation cleavage. The silty, non-crenulated samples show a somewhat narrower range for the I10 Å (0.5°) C/B intensity ratios, but a wider range for the c/b fissility ratios than do the finer-grained claystone/mudstone samples with an incipient crenulation cleavage.

4.4. Crystallographic preferred orientation

The preferred orientation of phyllosilicates was measured in transmission mode. The transmission geometry allows a maximum reduction of surface effects (Oertel, 1978), and this mode is recommended for phases with low 2θ diffraction angles, such as phyllosilicates.

Intensity data were measured on nine samples from the Helvetic Alps and 14 samples from the Swedish Caledonides using a pole-figure device. The data were corrected for background, irradiation volume, and absorption effects. The final values were normalized and weighted, and the intensities were expressed as multiples of a random distribution (mrd) after two smoothing cycles. The mrd is equivalent to a percentage of 1% area (Wenk, 1985). The orientation distributions were plotted on lower hemisphere equal-area projections. For the calculation of the March strain from the contour ellipses, the pole figures were rotated so that the maxima are oriented in the center of the plot (i.e. normal to cleavage, or to bedding if the maximum is parallel to bedding).

In all samples measurements were made from illite/muscovite (001) reflections (corresponding to $d = 10$ Å), the chlorite (001) reflections (corresponding to $d = 14$ Å), and the chlorite/kaolinite (002) reflections (corresponding to $d = 7$ Å). Prior to the orientation measurements, a full 2θ scan was made to determine the precise diffraction angles for these phases and to determine the background correction.

The results of the measurements of preferred orientation (after correction and smoothing) are listed in Table 2. The crystallographic preferred orientations of phyllosilicates (both mica and chlorite) change from bedding-parallel, to intermediate between cleavage and bedding, to parallel to cleavage. There are no differences between the preferred orientations of mica and chlorite in individual samples, but their intensities differ; Fig. 4 shows representative results (pole figure plots) (Table 3). The variations in both orientation and intensity of the various samples, and between the different regions, is remarkable. The maximum orientation intensities for all samples range from 2.35 to 12.91 for mica (001), from 2.86 to 16.71 for chlorite

Table 3
Maximum values and contour intervals for projections in Fig. 4

Sample No.	Mica (001)		Chlorite (001)		Chlorite/Kaolinite (002)	
	Max	Contour interval	Max	Contour interval	Max	Contour interval
Z91-1	7.08	0.67	7.99	0.78	7.85	0.78
Z91-2A	9.20	0.95	8.88	0.89	6.44	0.65
Z91-3	6.55	0.65	10.70	1.11	7.63	0.78
Z91-6	10.43	1.05	13.73	1.45	9.68	0.95
Z91-8	7.46	0.70	11.96	1.20	8.20	0.80
Z91-9	8.44	0.80	12.38	1.25	9.05	0.85
Z91-10	12.15	1.30	11.33	1.20	9.79	1.00
Z91-13	8.85	0.85	14.89	1.55	6.96	0.65
N78-44Bf	8.20	0.80	5.64	0.83	5.42	0.53
N78-47a	4.08	0.33	3.48	0.55	2.65	0.55
N78-59B	5.47	0.53	12.46	1.25	4.36	0.44
N92-15G	8.65	0.85	14.29	1.55	9.97	1.00

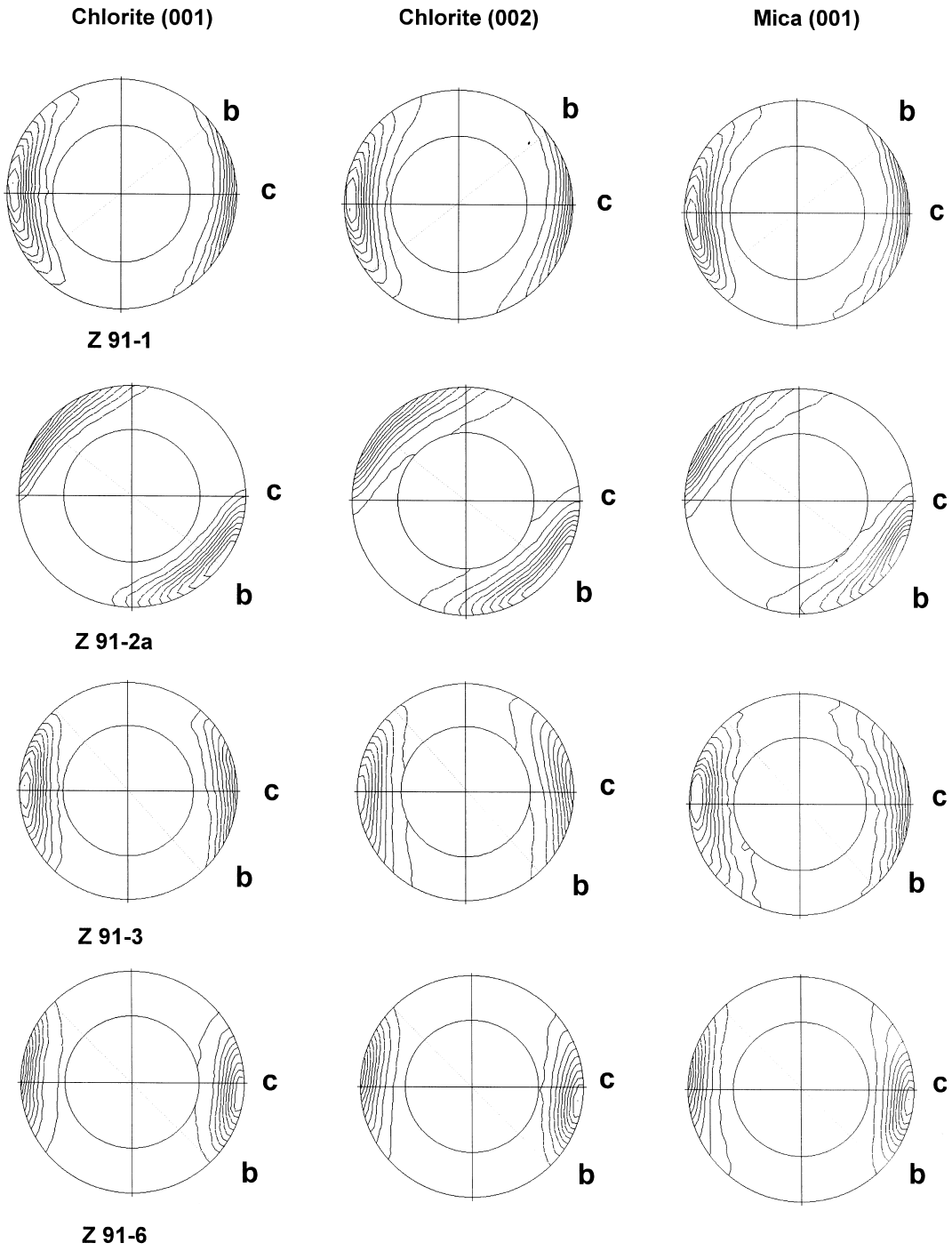

Fig. 4. Equal area projections of mica (001), and chlorite (001) and (002). Poles to cleavage and bedding are marked. No data can be obtained in the central area of the projections, due to the angular limitation of the transmission mode. Plots are contoured in multiples of random distribution (mrd). Maximum and contour intervals for each sample are listed in Table 3.

(001), and from 2.45 to 10.77 for chlorite/kaolinite (002). The orientation intensity strongly depends on the homogeneity, the lithological composition and the amount and size of detrital grains of the samples. The highest intensity values were obtained in samples where the intensity maxima (i.e. the phyllosilicates) are oriented parallel to the cleavage or in transition between bedding and cleavage. The high orientation intensities are characterized by high maximum count values, whereas some of the low orientation intensities

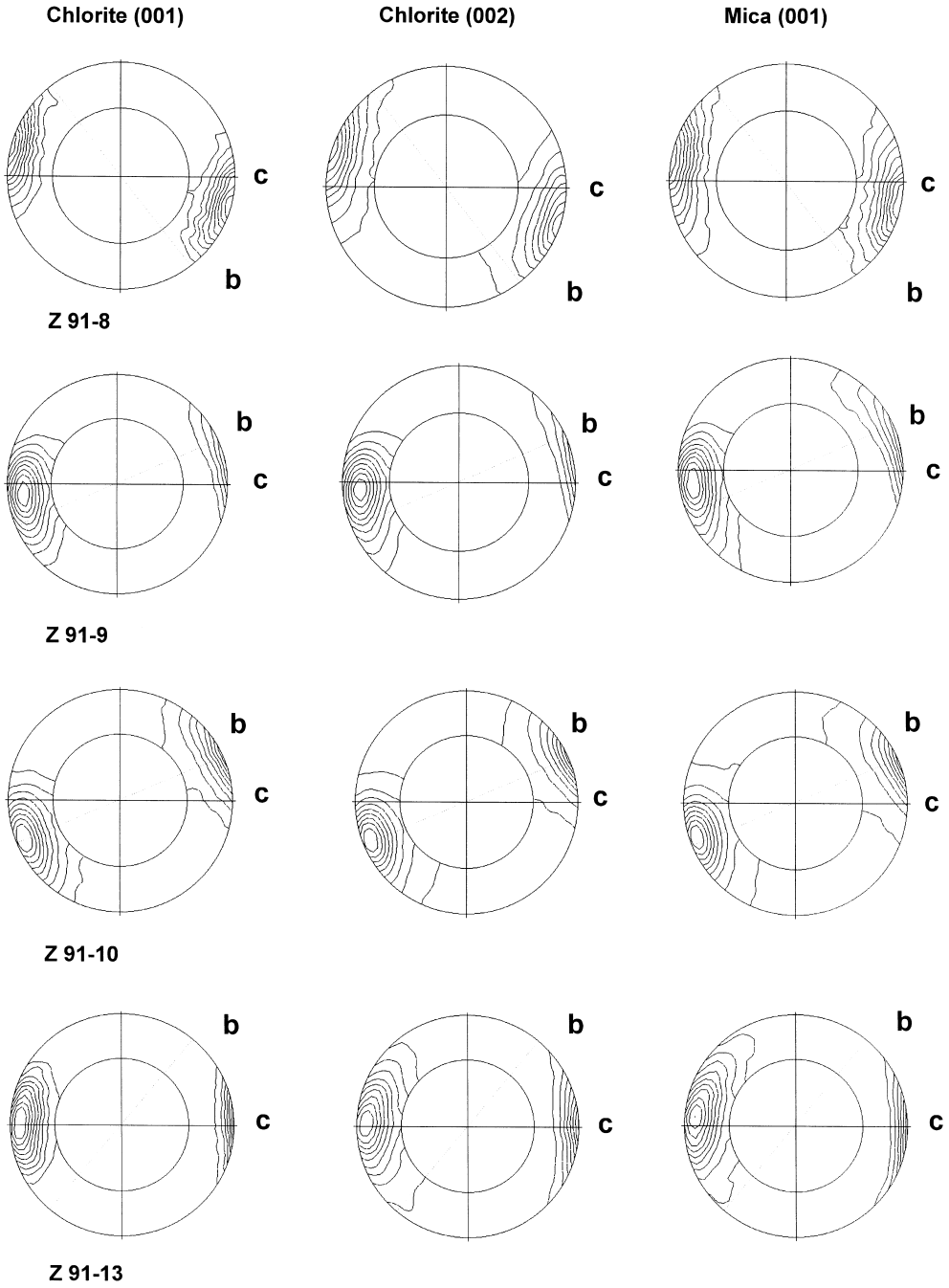

Fig. 4 (*continued*)

show very low count values in the maxima. Samples with mica and chlorite preferred orientation parallel to the cleavage generally show higher orientation maxima than those with a phyllosilicate preferred orientation parallel to the bedding planes. A difference in the intensities of the orientation maxima of the two regions is clear. The phyllosilicate preferred orientations in the samples of the Helvetic Alps are much stronger in intensity than in those of the Jämtland samples. In all samples from the Swiss Alps the phyllosilicate orientation is parallel to the cleavage or in between cleavage and bedding. The maximum intensities (in mrd) range from 6.55 to 12.91 for mica (001), from 7.99 to 16.71 for chlorite (001), and from 6.44 to 10.59 for chlorite/kaolinite (002).

The maximum intensities for the Jämtland samples are significantly lower than those of the Swiss samples. With few exceptions (N78-59B, N92-15G, N92-20) the phyllosilicates are oriented parallel to bedding. The intensity values range from 2.39 to 8.65 for mica (001),

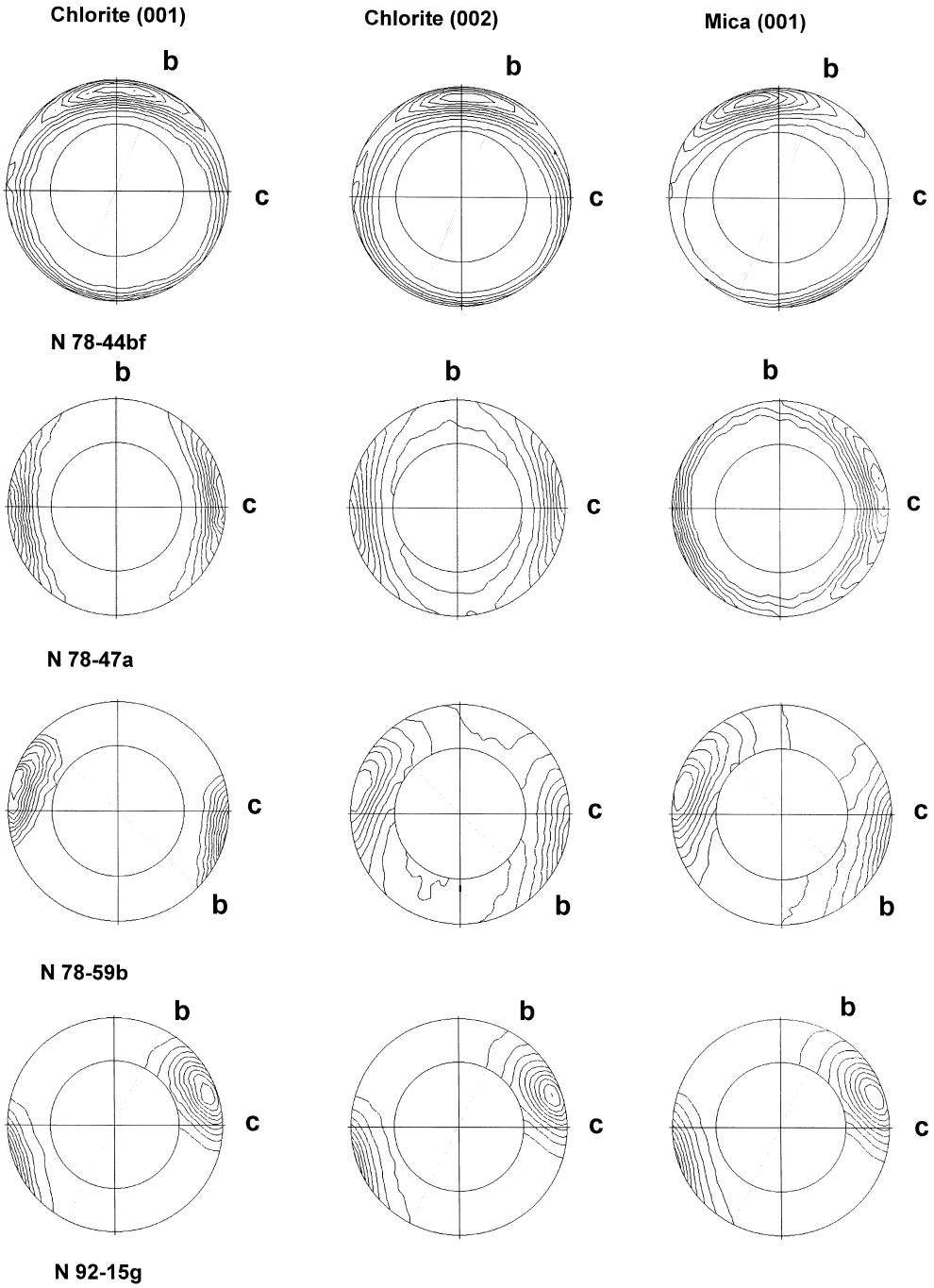

Fig. 4 (*continued*)

from 2.86 to 14.29 for chlorite (001), and from 2.45 to 9.97 for chlorite/kaolinite (002). Considering the phyllosilicate orientation, there is a trend to higher orientation values in samples with cleavage-parallel or transitional bedding/cleavage orientation (5.47 to 8.65 for mica (001), 5.64 to 14.29 for chlorite (001), 4.36 to 9.97 for chlorite/kaolinite (002), samples N78-44Bf, N78-59B, N92-15G, N92-20). The ranges for samples with bedding-parallel phyllosilicate preferred orientations are 2.39 to 4.22 for mica (001), 2.86 to 8.36 for chlorite (002), and 2.45 to 5.34 for chlorite/kaolinite (002). Sample N78-44Bg does not contain chlorite. In samples N92-6, N92-15F and N78-8A the chlorite (001) peak and the chlorite/kaolinite (002) peak, respectively, were not detected. In samples with bedding-parallel phyllosilicate preferred orientations (i.e. the samples with ill-defined maxima) the maximum orientation intensities of the mica (001) reflections are

connected with low numbers of counts in the maxima, whereas the samples with well-defined maxima result from larger numbers of counts (Table 2).

With few exceptions (Z91-2A, Z91-10, N78-44Bf), the chlorite preferred orientation is significantly stronger than that for mica. The orientation of the chlorite/kaolinite (002) reflections is weaker than that of the chlorite (001) reflections in most of the samples, but in most cases the absolute number of counts in the maxima of the (002) reflections is considerably higher than for the (001) reflections. With two exceptions the (001)/(002) intensity ratios range between 0.88 and 1.58. There is no obvious relationship between this ratio and the orientation of the maxima (parallel to cleavage or bedding).

4.5. March strains

The March model (March, 1932) has been used by several authors (Lisphie et al., 1976; Etheridge and Oertel, 1979; Curtis et al., 1980; Oertel, 1983; Chen and Oertel, 1991) to calculate principal preferred orientation densities and strains in some natural rocks. March (1932) considered the rotation of planes and lines during homogeneous deformation that affected all components of a given material. The elements in his model are passive markers which are reoriented by the strain. Thus the model represents an analytical relationship between strain and preferred orientation of markers. This relationship is subject to some assumptions:

- unimodal orientation distribution;
- constant volume;
- initially random distribution of markers;
- homogeneous deformation of both markers and matrix;
- March strain reflecting the total cumulative deformation of the sample from deposition onward.

Only few phyllosilicate-rich rocks fit these constraints, but some correlation with results of strain determinations on independent strain markers (Oertel, 1970; Tullis and Wood, 1975; Oertel et al., 1989) show that the strain values obtained by the March model are acceptable.

March (1932) derived a formula to describe the relationship between strain and preferred orientation:

$$e_i = \rho_i^{-1/3} - 1$$

where e_i is the principal strain, expressed as the ratio of the change of length to the original length, and ρ_i is a principal pole density of planar markers, normalized by dividing it by the average pole density for all orientations.

Orientations of the markers can be measured by pole figure analysis, and changes of orientations are reflected in changes of the pole figures.

March strain values and the parameters for the strain ellipsoid are listed in Table 4, and they are plotted in Fig. 5. This FLINN-plot (Flinn, 1962) is a graphical representation of the shape of strain ellipsoids made by plotting R_{yz} versus R_{xy} (Ramsay and Huber, 1983). The maximum March strains occur in the samples Z91-7, Z91-10 (Swiss) and N92-15G (Jämtland), and minimum values in the samples Z91-1 (Swiss), N78-5 and N78-18A, respectively. There are no significant differences in the trends of the strain values of mica and chlorite. In the FLINN-plot the values of mica and chlorite both plot in the field of axial shortening (apparent flattening) and the ellipsoids are all oblate. Therefore their intensities can be directly compared.

5. Discussion and conclusions

The samples of the Helvetic Alps are characterized by cleavage-parallel or -subparallel mica and chlorite preferred orientations, whereas most of the samples from the Swedish Caledonides show bedding-parallel phyllosilicate preferred orientations. That difference does not mean that the preferred orientation of phyllosilicates depends on the region or the structural relationship of the samples, but rather on the lithology, the cleavage morphology, and the deformation intensity of the analyzed rocks. The cleavage morphology and, consequently the phyllosilicate preferred orientation, are strongly affected by the lithology of the samples. Samples with bedding-parallel oriented phyllosilicates mainly show a domainal, discontinuous anastomosing cleavage. Mostly zonal or even discrete crenulation cleavage occurs in samples with cleavage-parallel, or in a transitional position between bedding- and cleavage-oriented micas and chlorites. The discontinuous anastomosing cleavage occurs in coarser-grained siltstones with a large number of clastic grains or chlorite/mica stacks (>50 μm) and in marly siltstones, whereas cleavage in finer-grained slates and silty mudstones with only few small clastic grains (<50 μm) appears as crenulation cleavage. The phyllosilicates in coarser-grained samples are mainly bedding parallel, and in finer-grained rocks, are either cleavage-parallel or are oriented at some intermediate angle to bedding and cleavage.

In contrast to the observations of Sintubin (1994b), the chlorite fabric intensities (with few exceptions) are higher than those of illite (Table 2), but do not always correspond to higher count numbers. Almost all samples show higher chlorite (001) intensity values, and about 50% of the samples show higher chlorite/kaolinite (002) intensity values. In contrast, only one

Table 4
March values from X-ray texture goniometry (calculated for mica (001) reflections)

Sample No.	e_1	e_2	e_3	X/Y	Y/Z	X/Z
parallel C						
Z91-1	0.62	0.19	−0.48	1.36	2.28	3.11
Z91-3	0.52	0.23	−0.47	1.23	2.31	2.84
Z91-6	0.68	0.30	−0.54	1.29	2.84	3.67
Z91-7	0.79	0.31	−0.57	1.37	3.07	4.21
Z91-13	0.61	0.28	−0.52	1.26	2.65	3.34
N78-59B	0.41	0.25	−0.43	1.12	2.21	2.48
N92-15G	0.53	0.34	−0.51	1.14	2.75	3.15
N92-20	0.46	0.34	−0.49	1.09	2.62	2.85
B–C						
Z91-2A	0.67	0.26	−0.52	1.33	2.63	3.50
Z91-8	0.48	0.32	−0.49	1.12	2.58	2.90
Z91-9	0.54	0.32	−0.51	1.16	2.69	3.13
Z91-10	0.64	0.40	−0.57	1.16	3.23	3.76
N78-44Bf	0.76	0.15	−0.50	1.54	2.31	3.55
parallel B						
N78-5	0.23	0.09	−0.25	1.13	1.45	1.64
N78-7	0.30	0.12	−0.31	1.16	1.62	1.88
N78-8A	0.31	0.09	−0.30	1.20	1.57	1.88
N78-44Bg	0.32	0.18	−0.35	1.12	1.82	2.03
N92-6	0.37	0.11	−0.34	1.23	1.70	2.08
N92-15D	0.28	0.11	−0.29	1.15	1.57	1.81
N92-15F	0.20	0.17	−0.29	1.03	1.63	1.68
N92-18A	0.18	0.14	−0.26	1.04	1.52	1.59
N92-18B	0.32	0.22	−0.38	1.09	1.97	2.14

sample has a higher chlorite (001) count number, and less than 50% of the samples have higher chlorite/kaolinite (002) count numbers. The orientation of chlorite–mica stacks in the coarser-grained samples, which reflects processes at the time of deposition, is a reason for the high intensity values of the chlorite-reflections, especially in samples with bedding-parallel phyllosilicate orientations. During crenulation cleavage development, the high degree of cleavage-parallel preferred orientation results in almost complete recrystallization and reorientation of fine-grained chlorite. In such samples the chlorite–mica stacks are mica-dominated and are highly deformed, mainly by rigid-body rotation and intragranular kinking (Fig. 1).

The March compaction strain ranges from 25% to 57%, which becomes narrower upon grouping different mica orientations. Compaction in samples with bedding-parallel mica preferred orientations ranges between 25% and 38%; March strain in samples with cleavage-parallel oriented micas, or with micas oriented between cleavage and bedding, ranges from 34% to 57%.

The FLINN-plot of our measurements shows a clear division into two clusters (Fig. 5):

I. samples with bedding-parallel oriented phyllosilicates;
II. samples with cleavage-parallel, or between cleavage- and bedding-oriented phyllosilicates.

The first cluster (I) represents pure compaction, whereas the second cluster (II) is a combination of compaction and tectonic strain. The first compactional strain episode is likely to be dominated by vertical shortening. Four of the Jämtland samples and all of the samples from the Helvetic Alps underwent further strain. Assuming a bedding-parallel first cleavage in the samples of the Alps (Kisch, 1998), finite strain in these rocks must be a combination of three elements: (a) compaction after the deposition; (b) development of a first, bedding-parallel cleavage; and (c) development of a second, non-bedding-parallel cleavage.

There are clear relationships between phyllosilicate preferred orientations and both X-ray diffraction intensity ratios and c/b fissility ratios. The degree of phyllosilicate preferred orientation of the samples with cleavage-parallel oriented phyllosilicates increases with

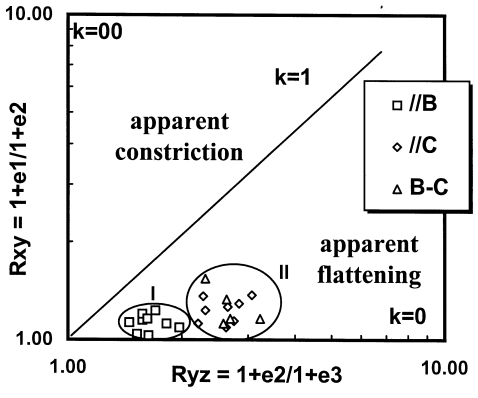

Fig. 5. Flinn diagram with pole figure patterns of samples with different phyllosilicate preferred orientations: parallel to bedding, parallel to cleavage, and in-between bedding and cleavage. See text for discussions.

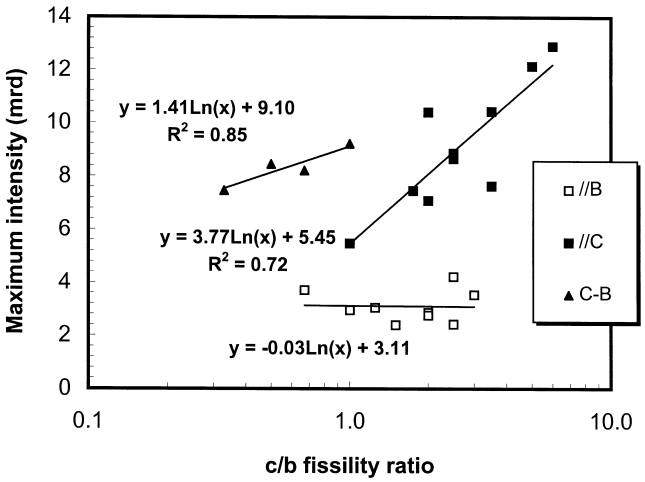

Fig. 6. Relationship between maximum intensities (mrd) of phyllosilicate preferred orientations and c/b cleavage/bedding fissility ratios.

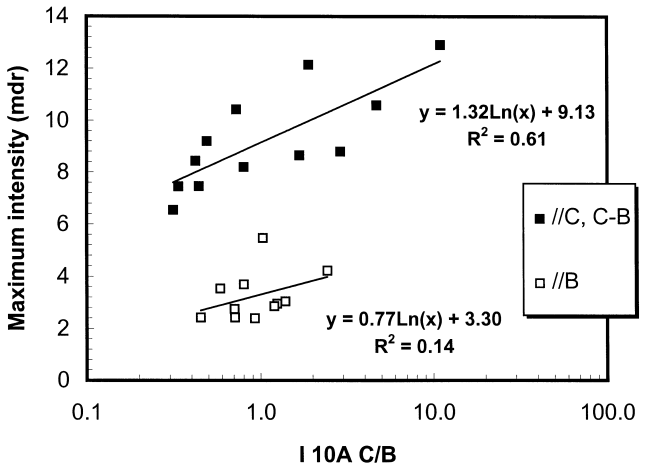

Fig. 7. Relationship between maximum intensities (mrd) of phyllosilicate preferred orientations and I10 Å (0.5°) C/B ratios.

increasing c/b fissility ratios, whereas the degree of preferred orientation remains essentially unchanged with increasing fissility ratios in samples with bedding-parallel phyllosilicate orientations (Fig. 6). This relationship is not unanticipated, because samples with cleavage-parallel oriented phyllosilicates show stronger cleavage and thus a better cleavage fissility. In contrast, bedding fissility is much better in samples with bedding-parallel preferred phyllosilicate orientations.

The relationship between phyllosilicate preferred orientations (mrd) and X-ray intensity ratios (I10 Å C/B) is shown in Fig. 7. The higher the maximum intensity ratios (mrd), so too, the higher the X-ray intensity ratios for samples with cleavage- and/or bedding-parallel preferred phyllosilicate orientations. In spite of the lower intensity values for samples with bedding-parallel phyllosilicates, the regression line is parallel to that of samples with cleavage-parallel or between cleavage- and bedding-oriented phyllosilicates. However, both relationships show considerable scatter.

With additional investigations on the influence of lithology and microtextural effects (cleavage morphology) it should be possible to quantify the cleavage intensity by determination of the X-ray intensity ratios. Measurements of fissility ratios after Durney and Kisch (1994) offer an excellent field method to get a reasonable estimate of cleavage intensity.

Acknowledgements

Special thanks are due to Nei-Che Ho for guidance with the X-ray goniometer at the University of Michigan, and Donald Peacor for discussions. We thank Carl Henderson for assistance with SEM analyses. Dida Banai and Esther Shani of the Department of Geology and Mineralogy, Ben-Gurion University of the Negev, and Beer-Sheva are thanked for their help with the X-ray diffraction analysis. Comments by Gerhard Oertel who reviewed the manuscript, and editorial handling by Joseph White are gratefully acknowledged. The studies were supported by the Deutsche Forschungsgemeinschaft (DFG) under grants Ja 754/2-1 and Ja 754/2-2. The single crystal XRD used in this study was acquired under grant EAR-89-17350, the SEM under grant EAR-96-28196, and fabric work is supported by EAR-96-14407 from the U.S. National Science Foundation.

References

Arkai, P., Balogh, K., Frey, M., 1997. The effects of tectonic strain on crystallinity, apparent mean crystallite size and lattice strain of phyllosilicates in low-temperature metamorphic rocks. A case study from the Glarus overthrust, Switzerland. Schweizerische Mineralogische und Petrographische Mitteilungen 77, 27–40.

Asklund, B., Thorslund, P., 1935. Stratigrafiska och tektoniska studier inom Föllingeområdet i Jämtland. Sveriges Geologiska Undersökning, Serie C, No. 388.

Chen, R.T., Oertel, G., 1991. Determination of March strain from phyllosilicate preferred orientation: a semi-numerical method. Tectonophysics 200, 173–185.

Curtis, C.D., Lisphie, S.R., Oertel, G., Pearson, M.J., 1980. Clay orientation in some Upper Carboniferous mudrocks, its relationship to quartz content and some inferences about fissility, porosity and compaction history. Sedimentology 27, 333–339.

Durney, D.W., Kisch, H.J., 1994. A field classification and intensity scale for first generation cleavages. AGSO Journal of Australian Geology and Geophysics 15, 257–295.

Etheridge, M.A., Oertel, G., 1979. Strain measurements from phyllosilicate preferred orientation—a precautionary note. Tectonophysics 60, 107–120.

Flinn, D., 1962. On folding during three dimensional progressive deformation. Quarterly Journal of the Geological Society, London 118, 385–428.

Gee, D.G., Kumpulainen, R., 1980. An excursion through the Caledonian Mountain Chain in central Sweden from Östersund to Storlien. Sveriges Geologiska Undersökning, Serie C, No. 774, Arsbok 74, No. 2, 1–66.

Gray, D.R., 1977. Morphologic classification of crenulation cleavage. Journal of Geology 85, 229–235.

Ho, N.-C., 1997. Preferred orientation development of phyllosilicates in diagenetic to greenschist facies environments, and related geological processes. Unpublished Ph.D. thesis, University of Michigan, 1–166.

Ho, N.-C., Peacor, D.R., van der Pluijm, B.A., 1995. Reorientation mechanisms of phyllosilicates in the mudstone-to-slate transition at Lehigh Gap, Pennsylvania. Journal of Structural Geology 17, 345–356.

Ho, N.-C., Peacor, D.R., van der Pluijm, B.A., 1996. Contrasting roles of detrital and authigenic phyllosilicates during slaty cleavage development. Journal of Structural Geology 18, 615–623.

Holleywell, R.C., Tullis, T.E., 1975. Mineral reorientation and slaty cleavage development in the Martinburg Formation, Lehigh Gap, Pennsylvania. Bulletin of the Geological Society of America 86, 1296–1303.

Kisch, H.J., 1980. Illite crystallinity and coal rank associated with lowest-grade metamorphism of the Taveyanne greywacke in the Helvetic zone of the Swiss Alps. Eclogae Geologicae Helvetiae 73, 753–777.

Kisch, H.J., 1990. Calibration of the anchizone: a critical comparison of illite "crystallinity" scales used for definition. Journal of Metamorphic Geology 8, 31–46.

Kisch, H.J., 1994. X-ray diffraction intensity ratios of phyllosilicate reflections in cleavage- and bedding-parallel slabs: incipient development of slaty cleavage in the Caledonides of Jämtland, western central Sweden. Revista Geológica de Chile 21, 253–267.

Kisch, H.J., 1998. Criteria of incipient slaty and crenulation cleavage development in Tertiary flysch of the Helvetic zone of the Swiss Alps. Journal of Structural Geology 20, 601–615.

Li, G., Peacor, D.R., Merriman, R.J., Roberts, B., van der Pluijm, B.A., 1994. TEM and AEM constraints on the origin and significance of chlorite–mica stacks in slates: an example from Central Wales, UK. Journal of Structural Geology 16, 1139–1157.

Lisphie, S.R., Oertel, G., Christie, J.M., 1976. Measurement of preferred orientation of phyllosilicates in schists. Tectonophysics 34, 91–99.

March, A., 1932. Mathematische Theorie der Regelung nach der Korngestalt bei affiner Deformation. Zeitschrift für Kristallographie 81, 285–297.

Milnes, A.G., Pfiffner, O., 1977. Structural development of the Infrahelvetic complex, eastern Switzerland. Eclogae geolicae Helvetiae 70, 83–95.

Oertel, G., 1970. Deformation of a slaty, lapillar tuff in the Lake District, England. Geological Society of America Bulletin 81, 1173–1188.

Oertel, G., 1978. The development of slaty cleavage in part of the French Alps—Discussion. Tectonophysics 47, 185–187.

Oertel, G., 1983. The relationship of strain and preferred orientation of phyllosilicate grains in rocks—a review. Tectonophysics 100, 413–447.

Oertel, G., Engelder, T., Evans, K., 1989. A comparison of the strain of crinoid columnals with their enclosing silty and shaly matrix of the Appalachian Plateau. Journal of Structural Geology 11, 975–993.

Pfiffner, O., 1978. Der Falten- und Kleindeckenbau im Infrahelvetikum der Ostschweiz. Eclogae geolicae Helvetiae 71, 61–84.

van der Pluijm, B.A., Ho, N.-C., Peacor, D.R., 1994. High-resolution X-ray texture goniometry. Journal of Structural Geology 16, 1029–1032.

Ramsay, J.G., Huber, M.I., 1983. The Techniques of Modern Structural Geology. Volume 1: Strain Analysis. Academic Press, London.

Sintubin, M., 1994a. Phyllosilicate preferred orientation in relation to strain path determination in the lower Paleozoic Stavelot–Venn Massif (Ardennes, Belgium). Tectonophysics 237, 215–231.

Sintubin, M., 1994b. Clay fabrics in relation to the burial history of shales. Sedimentology 41, 1161–1169.

Thorslund, P., 1940. On the Chasmops Series of Jemtland and Södermanland (Tväre n). Sveriges Geologiska Undersökning, Serie C, No. 436, 1–191.

Tullis, T.E., Wood, D.S., 1975. Correlation of finite strain from both reduction bodies and preferred orientation of mica in slate from Wales. Tectonophysics 78, 291–306.

Wenk, H.-R., 1985. Preferred orientation in deformed metals and rocks: An introduction to modern texture analysis. Academic Press, London.